

# Nonlinearity-assisted advantage for charger-supported open quantum batteries

Aparajita Bhattacharyya, Pratha Dongre, Ujjwal Sen

Harish-Chandra Research Institute, A CI of Homi Bhabha National Institute, Chhatnag Road, Jhansi, Prayagraj 211 019, India

We analyze the performance of a quantum battery in terms of energy storage and energy extraction, assisted by nonlinearities in a charger-battery system utilizing an open-system approach. In particular, we consider two types of nonlinearities in the system, viz. nonlinearity in the coupling between battery and charger, and the charger itself comprising an anharmonic oscillator. In both these scenarios, the charger is connected to an environment, and is driven by an external laser source. We derive the Markovian master equation for the dynamics of the combined charger-battery system in presence of the environment. When the charger is non-linearly coupled to a battery, we find an enhancement in the steady state ergotropy over the linearly-coupled case. We further see that the times at which steady state and maximum ergotropies are attained get decreased in presence of non-linear coupling. We also identify instances where no ergotropy is obtained in the linear case, but can be obtained in presence of any non-zero value of nonlinearity. We additionally find a complementarity between the non-linear interaction strength and the coherent-drive strength in the steady-state ergotropy values, i.e. the same ergotropy as that obtained using weak nonlinearity and strong coherent drive can be obtained utilizing an opposite order of their values. In case when the charger is modeled as a multi-level transmon with an inherent anharmonicity, we find an advantage in maximum ergotropy values over the harmonic instance. Unlike the non-linearly coupled batteries, the ones mediated by an anharmonic charger prove to be useful in the transient regime. We also determine values of the coherent drive for which the anharmonic battery is beneficial over the harmonic one at all timescales. Further, we observe a distinct region of the anharmonic strength and coherent drive where ergotropy values reach their maxima.

## I. INTRODUCTION

In the last two decades, there have been significant developments in quantum technologies, for instance, in transistors [1, 2], lasers [3] etc. which in the recent years have facilitated the study of individual quantum states and allowed us to manipulate systems exhibiting quantum properties such as superposition and entanglement. The major avenues of quantum technology that are currently achieving immense practical importance, are : quantum computation [4], quantum communication [5], quantum simulation [6] etc. This push towards the development of quantum technologies can be viewed from the perspective of two driving forces. Firstly, we identify that the increasing need to miniaturize technology has elicited the consideration of nontrivial effects of quantum mechanics. This emerging property calls for a new understanding of concepts in traditional thermodynamics, such as work, heat, and entropy [7–9]. The second motivation is the potential advantage achieved by harnessing quantum effects in certain applications, such as the enhancement of certain thermodynamic tasks in quantum machines, such as heat engines [10–12], refrigerators [13–15], and the quantum battery [16–18].

The storage of energy and subsequently extracting parts of the stored energy has become an important subject of study in quantum thermodynamics due to its practical importance [19–21]. The study of quantum batteries - quantum mechanical systems designed to store energy and extract it by harnessing quantum effects - has extensively been conducted in the recent years [22–26]. The extraction of this stored energy from a quantum battery by employing unitary processes has been extensively employed. The maximum amount of energy that can be withdrawn from a quantum battery using unitary operations is referred to as the ergotropy of the system [27]. The state of the system from which no further energy can be squeezed out, i.e., the states that cannot be further dis-

charged under unitary evolution, are called “passive” states. Such states are known to be diagonal in the energy eigenbasis of the Hamiltonian and ordered with decreasing eigenvalues corresponding to increasing energies.

Sophisticated theoretical proposals have been put forth that aim to increase the efficiency and performance of quantum batteries by exploiting inherent quantum advantage [28–35]. Previous work includes consideration of different realizations of the battery and charger, where the charger may interact with an environment, in presence of a coherent drive, and the energy of the battery gets affected due to its interaction with the charger. In [36], the authors have studied the various models of charger and battery in coherent and thermal charging settings and have concluded that when both the battery and charger are harmonic oscillators, the system always remains uncorrelated, and proven that the energy and ergotropy in such a scenario are the same. For harmonic oscillator charger and two level battery, they discovered that the time at which energy and ergotropy attain a maximum, decreases monotonically with the external driving field and also concluded that such a hybrid system - with a harmonic oscillator charger and a two level battery - facilitates faster charging of the battery over the situation where the charger and battery are not harmonic oscillator and two level system respectively. Previous analyses have further established the advantage of coherent charging in a hybrid system, i.e. a harmonic oscillator as charger and two-level system as battery, and have concluded that the time at which energy and ergotropy remain maximal decreases monotonically with the external driving field [36]. It has also been explored how a coherent drive affects the charging of such a hybrid battery, identifying that the coherent drive aids in increasing energy extraction efficiency [37].

Here we consider a quantum battery attached to an auxiliary system, which is referred to as the charger driven by an external driving source, and additionally interacts with an en-

vironment locally. This is to account for the fact that, realistically, when we only have access to the battery, the quantum effects can reduce the amount of energy converted to extractable work since some of the energy may be lost to correlations. We firstly consider the charger, which is a harmonic oscillator, to be coupled non-linearly to a two-level battery. In the second part, we consider anharmonicity in the charger system itself, while the two-level battery being connected linearly to the charger. We make the assumptions of Markovian evolution [38, 39] for the dynamics of the combined charger-battery system in presence of the environment. We identify instances where the nonlinearity assisted charging enhances the steady-state ergotropy, and facilitates faster achievement of maximum ergotropy. We also observe a complementary nature of the steady-state ergotropy values with respect to the non-linear interaction and the coherent drive strengths. In the anharmonicity-assisted charging, we find enhancement of the maximum ergotropy values, and find regimes of the coherent drive strength when the ergotropy is higher in the anharmonic case than that in the harmonic one at all timescales.

Anharmonic oscillator systems can be experimentally implemented using transmons. The system is characterized by a set of canonically conjugate quantum operators derived from the count of Cooper pairs moved through the junction and the phase difference across it. Charge-based systems are susceptible to stray electric field disturbances. This undesirable condition can be significantly mitigated by operating the Cooper pair box in the ‘‘transmon’’ regime, where the Josephson tunneling energy prevails over the Coulomb charging energy [40–42].

The remainder of the paper is arranged as follows. The relevant information necessary to formulate the problem is discussed in Sec. II. This includes a discussion on the quantum battery model that we consider, the master equation arising as a result of the interaction of the charger with the environment, and extraction of energy from quantum batteries. In Sec. III, the performance of quantum battery in energy extraction is provided, if the battery is non-linearly coupled to the charger. The dynamics of the charger-battery system, and its effects in energy extraction, in presence of anharmonic charger linearly coupled to a battery, is provided in Sec. IV. Finally, the concluding remarks are presented in Sec. V.

## II. PRELIMINARIES

In this section, we introduce the model that we consider, which comprises of a charger, battery, a bosonic environment and a coherent drive. We then provide a description of the Markovian master equations governing the dynamics of the joint system of charger and battery. We also discuss the prerequisites regarding energy extraction from quantum batteries using unitary operations.

### A. Quantum battery model

The model for charging a quantum battery and subsequent extraction of energy from it comprises of four distinct elements. The first element is a quantum battery,  $B$ , which is considered to be a qubit. The second element,  $A$ , is a quantum system referred to as the auxiliary, which acts as the charger. The third element,  $L$ , is the external energy supply of the model, which can be visualized as a classical laser source that injects energy into the battery through the auxiliary. In addition, the auxiliary,  $A$ , is kept in contact with a thermal reservoir,  $E$ , which is considered to be bosonic in nature. The charger and battery are described by their corresponding local Hamiltonians,  $H_A$  and  $H_B$ . They also interact with each other through an interaction,  $H_{AB}$ . The coherent laser source,  $L$ , is applied to the auxiliary at time  $t = 0$ , and the local modulating Hamiltonian of  $A$  due to  $L$  is given by  $\Delta H_A(t)$ . The Hamiltonian,  $H_{EA}$ , describes the interaction between the bosonic environment,  $E$  and the charger,  $A$ . So the global Hamiltonian of the composite system is given by

$$H = H_0 + \lambda(t)H_1, \quad (1)$$

where  $H_0 = H_A + H_B$  and  $H_1 = H_{AB} + H_{EA} + \Delta H_A(t)$ . The dimensionless quantity,  $\lambda(t)$ , takes value 1 when  $t \in [0, \tau]$ , and otherwise takes value zero. Physically it represents a classical parameter that acts as a switch and can be externally controlled to turn the interactions on and off. The two interaction terms,  $H_{AB}$  and  $H_{EA}$ , and the coherent drive,  $\Delta H_A(t)$ , are effective within the time period,  $[0, \tau]$ , after which they are all disconnected. The energy supplied by the laser to the auxiliary flows to the battery, because of the interaction between  $A$  and  $B$ . We consider the local Hamiltonians of  $A$  and  $B$  to commute with the coupling Hamiltonian,  $H_{AB}$ , i.e.  $[H_{AB}, H_A + H_B] = 0$ , which ensures that the evolution can only exchange energy between  $A$  and  $B$  and cannot increase or decrease the energy of the whole system.

We initially consider the charger to be a harmonic oscillator with energy difference between two consecutive levels being  $\omega_0$ . The battery is considered to be a single qubit, whose energy gap is exactly equal to the frequency of  $A$ . The frequency of the laser source is also considered to be  $\omega_0$ . The local Hamiltonians of  $A$  and  $B$ , and the modulating Hamiltonian of  $A$  due to  $L$  are given by

$$\begin{aligned} H_A &= K\tilde{\omega}\omega_0 a^\dagger a, \\ H_B &= K\frac{\omega_0}{2}(\sigma_B^z + 1), \\ \Delta H_A(t) &= K\sqrt{\tilde{\omega}}F(e^{-i\omega_0 t} a^\dagger + e^{i\omega_0 t} a). \end{aligned} \quad (2)$$

Here,  $a(a^\dagger)$  are the bosonic annihilation (creation) operators of the system,  $A$ , having the unit of  $1/\sqrt{\tilde{\omega}}$ . The parameter,  $K$ , has the dimension of energy and  $\omega_0$  is dimensionless. The dimensionless quantity,  $F$  represents the field strength corresponding to the coherent drive acting on  $A$ . Here  $\tilde{\omega}$  represents an arbitrary constant with the dimensions of frequency. The interaction between  $A$  and  $B$ , considering only linear order terms in  $a(a^\dagger)$ , is given by

$$H_{AB} = K\sqrt{\tilde{\omega}}g_1(a\sigma^+ + a^\dagger\sigma^-), \quad (3)$$

where  $g_1$  is the dimensionless linear-coupling constant between the systems  $A$  and  $B$ . A similar model for charging a quantum battery was considered in [43]. In our work, we incorporate nonlinearities in the interaction between  $A$  and  $B$  by introducing terms which are quadratic in the bosonic creation and annihilation operators. Such scenarios are physically realizable in several physical systems such as two-photon processes in superconducting circuits [44], trapped ion systems [45], etc. Previously, the effects of a two-photon process in a quantum battery has been considered, such as in [46, 47], although the main focus in these works was on closed system dynamics and in the absence of a charger.

## B. Interaction with the environment

The charger,  $A$ , interacts with a bosonic Markovian environment,  $E$ , and the interaction is described by the Hamiltonian,

$$H_{EA} = \int_0^{\omega_{max}} \sqrt{\tilde{\omega}} \hbar d\omega h(\omega) (a_\omega a^\dagger + a_\omega^\dagger a), \quad (4)$$

where the operators  $a_\omega^\dagger(a_\omega)$ , having the unit of  $1/\sqrt{\tilde{\omega}}$ , represents the bosonic creation (annihilation) operators corresponding to the mode  $\omega$  of the bath. Here  $\omega_{max}$  denotes the cutoff frequency of the bath. This cutoff frequency is set to be sufficiently high so that the memory time of the bath  $\sim \omega_{max}^{-1}$ , is negligibly small. This choice of parameters allows us to apply the Markovian approximations [38, 39, 48, 49]. Here  $h(\omega)$  is a dimensionless function of  $\omega$ , that tunes the coupling between the harmonic oscillator and environment. The local Hamiltonian describing the bath is given by

$$H_E = \int_0^{\omega_{max}} \hbar \tilde{\omega} a_\omega a_\omega^\dagger d\omega. \quad (5)$$

For harmonic oscillator baths,  $\tilde{\omega} h^2(\omega) = J(\omega)$ , where  $J(\omega)$  represents the spectral density function of the bath. In this paper, we have taken  $J(\omega)$  to be the Ohmic spectral density function having the form  $J(\omega) = \alpha \omega \exp(-\omega/\omega_{max})$ . Here  $\alpha$  represents the dimensionless interaction strength between the harmonic-oscillator charger and the bosonic bath.

Each of  $A$  and  $B$  are assumed to be initially prepared in the ground states of their respective Hamiltonians, denoted by  $|0\rangle\langle 0|_A$  and  $|0\rangle\langle 0|_B$ , such that the joint charger-battery initial state is  $\rho_{AB}(t=0) = |0\rangle\langle 0|_A \otimes |0\rangle\langle 0|_B$ . The quantity,  $|0\rangle\langle 0|_B$  is simply the ground state of the Hamiltonian,  $H_B$ , whereas  $|0\rangle\langle 0|_A$  represents the ground state of the operator,  $\omega_0 a^\dagger a$ . As we turn on the dissipation between  $A$  and  $E$ , the coherent drive,  $\Delta H_A$ , and the interaction between  $A$  and  $B$ , the joint system of  $EAB$  evolves unitarily under the global Hamiltonian,  $H$ , following which, the environment is discarded. Since the initial system-environment state - the system comprising the charger and battery - is product, and a global unitary acts on the entire system-environment state, followed by tracing out the environment, the evolution of the system can be effectively considered to be a completely positive

trace preserving (CPTP) operation. Moreover, Markovian approximations are made while considering such a CPTP operation on the charger and battery. Therefore the dynamics of the combined state of the battery and charger is governed by the the Gorini-Kossakowski-Sudarshan-Lindblad (GKSL) master equation. Throughout the process, energy is transferred between  $A$  and  $E$ , and due to the interaction between  $A$  and  $B$ , energy is also exchanged between  $A$  and  $B$  as well. As a result, the dynamics of  $B$ , considered separately, becomes non-Markovian in nature.

To simplify the analysis of the system dynamics, we move to the interaction picture representation. The resultant density matrix of  $A$  and  $B$  at time  $t$ , given by  $\tilde{\rho}_{AB}(t)$  in the interaction picture, is

$$\tilde{\rho}_{AB}(t) = e^{i(H_A+H_B)\tilde{t}/\hbar} \rho_{AB}(\tilde{t}=0) e^{-i(H_A+H_B)\tilde{t}/\hbar}. \quad (6)$$

Here,  $t$  denotes the dimensionless time with the actual time  $\tilde{t}$ , defined as  $t = \frac{K\tilde{t}}{\hbar}$ . In the interaction picture, the evolution of such a system within the time period,  $t \in [0, \tau]$ , is governed by the following master equation

$$\dot{\tilde{\rho}}_{AB}(t) = \mathcal{L}_{AB}[\tilde{\rho}_{AB}(t)], \quad (7)$$

where  $\mathcal{L}_{AB}$  is the GKSL super-operator [49–53]. The term,  $\mathcal{L}_{AB}[\dots]$ , can explicitly be written as

$$\begin{aligned} \mathcal{L}_{AB}(t)[\tilde{\rho}_{AB}(t)] = & -i \frac{1}{K} [\Delta H_A(t) + H_{AB}, \tilde{\rho}_{AB}(t)] \\ & + \frac{\hbar}{K} \mathcal{D}[\tilde{\rho}_{AB}(t)], \end{aligned} \quad (8)$$

where the first term on the right hand side of Eq. (8) represents the unitary part, whereas the second term is the non-unitary dissipator term. The dynamical equation for the joint system  $AB$ , is described by the GKSL master equation, as presented in Eq. (7), with the dissipative term given by

$$\begin{aligned} \mathcal{D}[\tilde{\rho}_{AB}(t)] = & \sum_{\omega'} \gamma(\omega') \left[ L^{\omega'} \tilde{\rho}_{AB}(t) L^{\omega'\dagger} \right. \\ & \left. - \frac{1}{2} \{ L^{\omega'\dagger} L^{\omega'}, \tilde{\rho}_{AB}(t) \} \right], \end{aligned} \quad (9)$$

with  $i = 1, 2$ . The quantity,  $\gamma(\omega')$  denotes the dimensionless decay constant, where  $\tilde{\gamma}(\omega') = \frac{\hbar \gamma(\omega')}{K}$ . The operators,  $L_i^{\omega'}$  represent the Lindblad or jump operators associated with the possible transition frequencies  $\omega'$  of the joint state of  $A$  and  $B$ . In the Markovian master equation, the information of the reservoirs is embedded in the transition rates or decay constants,  $\{\tilde{\gamma}(\omega')\}$ , which is given by

$$\begin{aligned} \tilde{\gamma}(\omega') = & J(\omega') [1 + f(\omega', \beta)] & \omega' > 0 \\ = & J(|\omega'|) f(|\omega'|, \beta) & \omega' < 0, \end{aligned} \quad (10)$$

where  $f(\omega', \beta) = [\exp(\beta \hbar \omega') - 1]^{-1}$  is the Bose-Einstein distribution function for the bosonic heat bath. The joint evolution of the charger and battery can be described by the Markovian master equation given in Eq. (7), by solving which, one can obtain the density operator,  $\tilde{\rho}_{AB}(t)$ , as a function of time. Following this, the auxiliary is traced out to obtain the dynamics of the battery,  $B$ , alone. Therefore, the evolution of the battery, considered separately, is in general, not Markovian in nature.

### C. Energy extraction using unitaries

A quantum battery is a quantum mechanical system characterized by a density matrix and a Hamiltonian. The system can be charged by applying some unitary or non-unitary operations on it. Once it is charged, our aim is to extract maximum possible energy from the battery. The maximum extractable energy from a quantum battery, under unitary operations, is referred to as the ergotropy of the battery. After the extraction of maximum amount of energy from the battery, the states from which no further energy can be extracted are termed as passive states. In other words, passive states are states from which energy extraction is not possible using unitary operations. Passive states are important in the framework of quantum batteries or, more generally, in quantum thermodynamics [54–58].

In the case that we consider, the charger interacts with the coherent laser source and also with the environment, as a result of which average energy of the charger varies in the time interval,  $[0, \tau]$ . Further, due to the interaction of the charger with the battery, exchange of energy occurs between  $A$  and  $B$  as well. Therefore, as the laser injects energy into the auxiliary, the battery also gets charged due to the presence of the interaction,  $H_{AB}$ , in the time interval  $[0, \tau]$ . The average energy contained in  $B$  at the end of the charging process is  $E_B(\tau) = \text{tr}[H_B \rho_B(\tau)]$ . Our aim is to extract the maximum energy from  $\rho_B(\tau)$  using unitary operations. The ergotropy,  $\varepsilon_B(\tau)$ , in such a case, is mathematically given by

$$\begin{aligned} \varepsilon_B(\tau) &= \text{Tr}(\rho_B(\tau)H_B) - \min_U \text{Tr} [U(\lambda)\rho_B(\tau)U(\lambda)^\dagger H_B], \\ &= \text{Tr}(\rho_B(\tau)H_B) - \text{Tr}(\rho_B^{(p)} H_B) \\ &= E_B(\tau) - E_B^{(p)}(\tau), \end{aligned} \quad (11)$$

where the first term on the right-hand side of the last equation represents the average energy of  $\rho_B$  at time  $\tau$ , and the quantity,  $E_B^{(p)}(\tau) = \text{tr}[H_B \rho_B^{(p)}(\tau)]$ , is the energy of the passive state,  $\rho_B^{(p)}$  corresponding to state  $\rho_B$ . So the amount of energy contained in the passive state,  $\rho_B^{(p)}$ , is “forbidden”, in the sense that, this energy cannot be extracted from  $\rho_B(\tau)$ , for the given  $H_B$  and would be left in the system after extracting all the unitarily accessible energy from  $\rho_B(\tau)$ . The necessary and sufficient conditions for a state,  $\rho_B^{(p)}$ , to be passive are that it should commute with its Hamiltonian,  $H_B$ , and if for a particular order of the eigenvectors the corresponding eigenvalues of  $H_B$ ,  $\{\epsilon_i\}_i$ , satisfy  $\epsilon_i > \epsilon_j$ , then the eigenvalues of the passive state,  $\{\lambda\}_i$ , should satisfy  $\lambda_i \leq \lambda_j$  for all  $i$  and  $j$  [59, 60].

### III. ENERGY EXTRACTION ASSISTED BY NON-LINEARLY COUPLED SYSTEM AND CHARGER

In the field of cavity and circuit quantum electrodynamics, it is possible to implement effective two-level quantum systems, viz. superconducting qubits, interacting with bosonic modes supported by microwave sources. Nonlinearities may

arise in such circuits between a flux qubit and a bosonic mode supported by a superconducting quantum interference device [44]. We here analyze the maximum extractable energy from quantum batteries when a charger couples with a battery using such nonlinear interactions. The corresponding interaction Hamiltonian comprising the charger and battery is as follows

$$H_{AB} = K\sqrt{\tilde{\omega}}g_1(a\sigma^+ + a^\dagger\sigma^-) + K\tilde{\omega}g_2(a^2\sigma^+ + (a^\dagger)^2\sigma^-), \quad (12)$$

where  $g_2$  is the dimensionless coupling constant between systems A and B associated with the non-linear interaction. The interaction of the charger with the environment is given by Eq. (4). The terms  $H_A, H_B$  and  $H_{AB}$  contribute to the unitary evolution of the system, whereas the interaction of system A with the environment gives rise to the GKSL type dissipative terms. The resultant master equation is of the following form

$$\begin{aligned} \dot{\rho}_{AB}(t) &= -i[\sqrt{\tilde{\omega}}g_1(a\sigma^+ + a\sigma^-) \\ &\quad + \tilde{\omega}g_2(a^2\sigma^+ + (a^\dagger)^2\sigma^-) \\ &\quad + \sqrt{\tilde{\omega}}F(a^\dagger + a), \tilde{\rho}_{AB}(t)] \\ &\quad + J(\omega_0)(1+f)\left[a\tilde{\rho}_{AB}(t)a^\dagger - \frac{1}{2}\{a^\dagger a, \tilde{\rho}_{AB}(t)\}\right] \\ &\quad + J(\omega_0)f\left[a^\dagger\tilde{\rho}_{AB}(t)a - \frac{1}{2}\{aa^\dagger, \tilde{\rho}_{AB}(t)\}\right], \end{aligned} \quad (13)$$

where  $J(\omega_0) = \alpha\omega_0 \exp(-\omega_0/\omega_{max})$  and  $f = f(\omega_0, \beta) = [\exp(\beta\hbar\omega_0) - 1]^{-1}$  are the Ohmic spectral density function and the Bose-Einstein distribution function respectively. For solving the differential equations, we employ numerical methods using C++, adhering to the truncation of the annihilation and creation operators for studying the evolution of the system for a finite duration of time. In this paper, we have truncated the oscillators up to 10 levels. While truncating the matrices, it has been ensured that the differences in the higher eigenvalues become relatively small, and the relevant physical quantities converge for the energy-level cut-off chosen.

After solving the master equation for  $\tilde{\rho}_{AB}(t)$ , we discard the charger and calculate the ergotropy of the battery using Eq. (11). In Fig. 1, we plot the steady-state ergotropy along the vertical axis versus the non-linear coupling strength along the horizontal axis, as represented by the yellow solid curve. The solid yellow curve corresponds to  $\tau = 120$  when steady state has been attained. We find that the steady state ergotropy is non-zero in the absence of the non-linear interaction, and as we turn on the interaction, it gradually increases with an increase in the non-linear coupling strength,  $g_2$ . So nonlinearity helps in obtaining higher ergotropy at steady states. The plot in Fig. 1 is given for a fixed value of the coherent drive,  $F = 0.5$ . However, this feature of obtaining higher ergotropy at steady states has been observed within a wide range of the coherent drive, viz  $0.5 \leq F \leq 1.5$ . The linear coupling strength is considered to be  $g_1 = 0.1$ . So we see that there is an advantage over the linear case both in the regimes of weak and strong non-linear coupling, i.e.  $g_2$  is close to 0 and 0.1 respectively. Moreover, we find that there exists a time,  $\tau = 30$ , when no energy can be extracted from the battery resulting in zero ergotropy in the linear coupling case, but the maximum

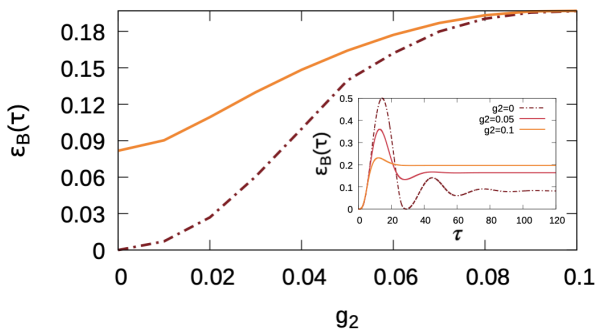


Figure 1. Demonstration of ergotropy,  $\varepsilon_B(\tau)$ , of the quantum battery along the vertical axes with respect to the non-linear coupling strength,  $g_2$ , along the horizontal axis. The field strength corresponding to the coherent drive is  $F = 0.5$ , and the linear coupling strength is  $g_1 = 0.1$ . The solid yellow and brown dotted-dashed curves correspond to  $\tau = 120$  and  $\tau = 30$  respectively. **Inset:** Depiction of the maximum extractable energy versus time for different values of non-linear interaction strength,  $g_2$ . The coherent drive strength and the linear coupling strength is same as in the main figure. Both in the main figure and inset, the quantities plotted along the horizontal axis is dimensionless, while ergotropy is units of  $K$ .

extractable energy at that time corresponding to non-linear coupling with any positive coupling strength is non-zero. This is depicted by the dotted-dashed curve in Fig. 1. In the ergotropy versus time graph, as provided in the inset of Fig. 1, we observe that the oscillatory behavior of  $\varepsilon_B(\tau)$  is reduced with nonlinearity. There is a loss in the maximum ergotropy attained using non-linear coupling, however there is a faster attainment of the steady state. The battery interacts with the Markovian bath through the charger, and increased non-linear coupling between the battery and charger reduces the effective correlation of the battery with the bath, resulting in less decay of maximum extractable energy in the steady state regime. So, if in any setup, there is a need of energy extraction continuously for a long time, then the nonlinearity assisted coupling between the battery and charger proves to be beneficial.

Now, if we increase the strength of the coherent drive, then for fixed value of drive, we find that the peak in the ergotropy versus time plot, i.e. the point where maximum ergotropy is attained, shifts to the left along the horizontal axis, as we increase the non-linear interaction strength. The actual value of ergotropy, with or without non-linear coupling, increases with an increase in the coherent drive, however the steady state value drops. We represent the time at which maximum ergotropy is attained by  $\tau_m$ . In the inset of Fig. 2, we plot  $\tau_m$  versus the non-linear interaction strength,  $g_2$ . We find that, with an increase in the nonlinearity in the system-charger coupling, the maximum ergotropy is attained faster. So, if there is a requirement of large amount of energy extraction at small timescales, then non-linear coupling between the battery and charger proves to be advantageous. However, when compared with the peak when there is no nonlinearity in the model, i.e. when  $g_2 = 0$ , we observe that the maximum ergotropy of the linear model is higher than that of the non-linearly coupled model which is reflected in Fig. 2. The qualitative behavior

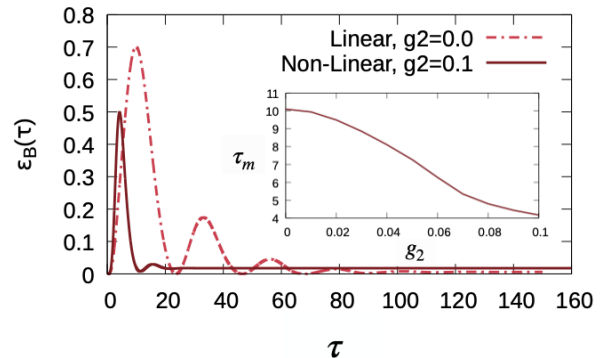


Figure 2. Depiction of ergotropy of the battery,  $\varepsilon_B(\tau)$ , corresponding to non-linear and linear coupling of the battery with the charger, represented by solid and dotted curves respectively along the vertical axis, which is plotted against interaction time,  $\tau$  along the horizontal axis. The field strength corresponding to the coherent drive is  $F = 1.5$ , and the linear coupling strength is  $g_1 = 0.1$ . The quantities plotted along the horizontal axis is dimensionless, while ergotropy is in units of  $K$ . **Inset:** Demonstration of the time at which the maximum ergotropy is attained, given by  $\tau_m$  along the vertical axis, with respect to non-linear coupling strength,  $g_2$  along the vertical axis. Quantities plotted along both axes are dimensionless.

of energy versus time plot is also similar. With increasing strength of the driving amplitudes, there is a clear decrease of the time required to attain the maximum energy.

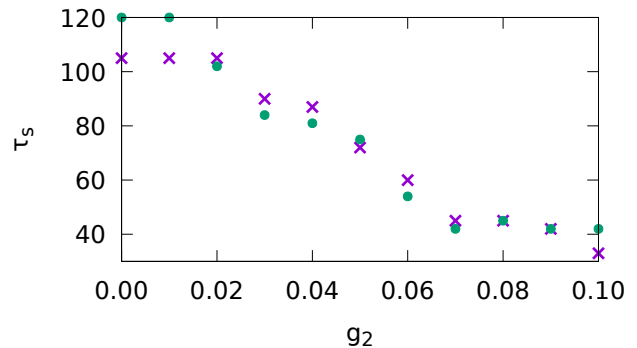


Figure 3. The time  $\tau_s$  at which the ergotropy,  $\varepsilon_B(\tau)$ , and energy,  $E_B(\tau)$ , reaches their steady state values, as represented by teal circles and purple crosses respectively, which are plotted along the vertical axis, versus the non-linear interaction strength plotted along the horizontal axis. Here we have obtained the results by setting  $g_1 = 0.1$ ,  $\gamma = 1.0$ ,  $F = 0.5$ , and we have set inverse temperature  $\beta = 1$ . The quantities plotted along both the axes are dimensionless.

In Fig. 1, we see that the the steady-state ergotropy increases with an increase in the non-linear interaction strength between charger and battery. Moreover, the time of attainment of steady state also becomes less as the nonlinearity is increased. In Fig. 3, we plot the time where steady-state is reached, given by  $\tau_s$ , along the vertical axis versus the non-linear strength,  $g_2$ , along the horizontal axis. We find that,

with an increase in nonlinearity, the steady state is reached faster. So if there is a requirement of steady source of energy at comparatively small times, then the utility of nonlinearity in the interaction between charger and battery proves to be useful.

Having seen that for lower values of the coherent drive, higher non-linear coupling strength gives a higher steady state ergotropy. Intrigued by this feature, we ask what happens to the steady-state ergotropy if we increase the strength of the coherent drive. We find a complementarity between strengths of the nonlinear interaction,  $g_2$ , and the coherent drive,  $F$ , for obtaining the same steady-state ergotropy values. Specifically we find that higher values of ergotropy are obtained in the scenarios when the value of  $g_2$  is low and that of  $F$  is high, or vice versa. The optimal value of steady-state ergotropy is found when both the non-linear coupling strength and coherent drive strength are intermediate. Refer to Fig. 4 for this. Therefore, higher values of the non-linear coupling strength result in higher steady-state values, even for low values of coherent drive strength.

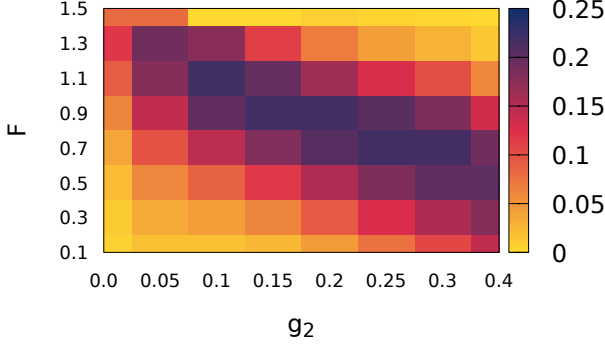


Figure 4. Depiction of the steady state value of ergotropy obtained for different values of the coherent drive intensity  $F$  along the vertical axis, and the non-linear coupling strength,  $g_2$ , along the horizontal axis. The quantities plotted along the horizontal and vertical axes are dimensionless, while ergotropy is in units of  $K$ .

We found scenarios when nonlinearity in the coupling between battery and charger assists the availability of maximum extractable energy in the steady state. Further, we found instances where the availability of maximum ergotropy and steady state ergotropy is facilitated at a lesser time, due to the presence of non-linear interactions between charger and battery.

#### IV. ENERGY EXTRACTION ASSISTED BY ANHARMONIC CHARGER

In this section, we analyze the discharging of a quantum battery interacting with a bosonic Markovian environment through a charger, which is considered to be a transmon. We begin by considering the Hamiltonian of a quantum harmonic oscillator, which is obtained by quantizing the Hamiltonian of an  $LC$  circuit, where  $L$  refers to inductance and  $C$

is the capacitance. This Hamiltonian is usually applicable in superconductivity-based systems such as the Cooper-pair box [61]. The quantized Hamiltonian is given by,

$$\hat{H}_{HO} = \frac{\hat{Q}^2}{2C} + \frac{\hat{\Phi}^2}{2L}, \quad (14)$$

where  $\hat{Q}$  refers to the charge variable and  $\hat{\Phi}$  is the flux variable. These operators satisfy the following commutation relation,

$$[\hat{\Phi}, \hat{Q}] = i\hbar, \quad (15)$$

where  $\hbar = h/2\pi$ , and  $h$  is the Planck's constant. The Hamiltonian is written in a more recognizable form by introducing the reduced charge,  $\hat{n} = \hat{Q}/2e$ , where  $2e$  is the charge content of a Cooper pair, and the phase  $\hat{\phi} = 2\pi\hat{\Phi}/\phi_0$ , where  $\phi_0 = h/2e$  is the flux quanta. Using this notation the Hamiltonian reduces to the form

$$\hat{H}_{HO} = 4E_c\hat{n}^2 + \frac{1}{2}E_L\hat{\phi}^2, \quad (16)$$

where  $E_c = e^2/2C$  is the charging energy and  $E_L = (\phi_0/2\pi)^2/L$  is the inductive energy.

Coupling two superconducting islands, or alternatively, an island and a ground through a Josephson junction [62] is the standard set-up for a transmon. The effective Hamiltonian of the Cooper-pair box in the transmon regime can be written as [62–64]

$$\hat{H} = 4E_c\hat{n}^2 - E_J \cos \hat{\phi}, \quad (17)$$

where  $E_J = I_0\phi_0/2\pi$  is the Josephson energy. The current  $I$  and flux  $\Phi$ , across the Josephson junction are connected by the relation,  $I = I_0 \sin(2\pi\Phi/\Phi_0)$ . Here we see that the phase is not in the form for that of a linear inductor. This is due to the presence of a Josephson junction. We now express the charge and phase operators in terms of annihilation and creation operators of the transmon. The charge operator,  $\hat{n}$  and phase operator,  $\hat{\phi}$  are respectively given by

$$\hat{n} = i \left( \frac{E_J}{32E_c} \right)^{1/4} (\hat{b}^\dagger - \hat{b}), \quad \hat{\phi} = \left( \frac{2E_c}{E_J} \right)^{1/4} (\hat{b}^\dagger + \hat{b}). \quad (18)$$

Here  $\hat{b} = \sum_n \sqrt{n+1}|n\rangle\langle n+1|$  is the annihilation operator of the transmon, and unlike the harmonic oscillator, the energy modes are not evenly spaced. In the transmon regime, the Josephson and inductive energies hold the following inequality:  $\beta = E_J/E_c \gg 1$ . This allows one to take a Taylor expansion of  $\cos \hat{\phi}$  and approximate the Hamiltonian to obtain

$$\begin{aligned} \hat{H} = & -4E_c \sqrt{\frac{\beta}{32}} (\hat{b}^\dagger - \hat{b})^2 \\ & - E_J \left( 1 - \frac{1}{2} \sqrt{\frac{2}{\beta}} (\hat{b}^\dagger + \hat{b})^2 + \frac{1}{12\beta} (\hat{b}^\dagger + \hat{b})^4 + \dots \right), \\ \approx & \sqrt{8E_c E_J} \left( \hat{b}^\dagger \hat{b} + \frac{1}{2} \right) - E_J - \frac{E_c}{12} (\hat{b}^\dagger + \hat{b})^4. \end{aligned} \quad (19)$$

Performing the rotating wave approximation and then defining  $\omega' = \sqrt{8E_c E_J}$  and the anharmonicity of the transmon as  $\delta = -E_c$ , we obtain

$$\hat{H} = \left(\omega' + \frac{\delta}{2}\right) \hat{b}^\dagger \hat{b} + \frac{\delta}{2} (\hat{b}^\dagger \hat{b})^2. \quad (20)$$

We consider the charger to be an anharmonic oscillator represented by the transmon. The battery is a two-level system as considered in the previous section. The charger interacts with a bosonic Markovian environment,  $E$ , through an interaction hamiltonian  $H_{EA}$ . The Hamiltonian of the transmon charger is the same as  $\hat{H}$ . The total Hamiltonian involving the charger and environment is given by

$$\tilde{H} = \tilde{H}_A + \tilde{H}_E + \tilde{H}_{EA}, \quad (21)$$

where  $\tilde{H}_A = K\tilde{\omega}\tilde{\omega}_0 b^\dagger b - K\tilde{\omega}^2\tilde{\omega}_1 (b^\dagger b)^2$ , and  $\tilde{H}_E = H_E$  as defined in Sec. II B. Here  $b(b^\dagger)$  are the annihilation (creation) operators of the transmon charger, having the unit of  $1/\sqrt{\tilde{\omega}}$ . The operators  $a_\omega^\dagger(a_\omega)$ , having the unit of  $1/\sqrt{\tilde{\omega}}$ , represents the bosonic creation (annihilation) operators corresponding to the mode  $\omega$  of the bath. The notations,  $K$ ,  $\tilde{\omega}$  have their same meanings as in Sec. II, and the dimensionless quantities,  $\tilde{\omega}_0$  and  $\tilde{\omega}_1$  have their magnitudes equal to  $(\omega' + \delta/2)$  and  $-\delta/2$  respectively.

The interaction between the system  $A$  and the bath is given by

$$\tilde{H}_{EA} = \int_0^{\omega_{max}} \sqrt{\tilde{\omega}} \hbar d\omega \tilde{h}(\omega) (b^\dagger a_\omega + b a_\omega^\dagger), \quad (22)$$

where  $\tilde{h}(\omega)$  denotes the strength of the coupling between the charger  $A$  and the environment. The interaction between the charger and the environment, i.e.  $H_{EA}$ , can be rewritten as a sum of the tensor product of Hermitian operators corresponding to the charger and the bath, given by  $H_{EA} = \sum_{i=1}^2 A_i \otimes B_i$ , where  $A_i$  and  $B_i$  for  $i = 1$  to  $2$  are the operators corresponding to the charger  $A$ , and the bath  $B$  respectively. In the case that we consider, the system operators are of the form

$$A_1 = b^\dagger + b, \quad A_2 = i(b^\dagger - b), \quad (23)$$

The bath operators, denoted by  $B_i$ , for  $i = 1$  and  $2$  are given by

$$B_1 = \int_0^{\omega_{max}} d\omega h(\omega) \frac{(a_\omega + a_\omega^\dagger)}{2} = \int_{-\omega_{max}}^{\omega_{max}} d\omega B_1(\omega),$$

$$\text{where } B_1(\omega) = h(\omega) \frac{a_\omega}{2} \text{ and } B_1(-\omega) = h(\omega) \frac{a_\omega^\dagger}{2},$$

$$B_2 = \int_0^{\omega_{max}} d\omega h(\omega) \frac{i(a_\omega^\dagger - a_\omega)}{2} = \int_{-\omega_{max}}^{\omega_{max}} d\omega B_2(\omega),$$

$$\text{where } B_2(\omega) = -ih(\omega) \frac{a_\omega}{2} \text{ and } B_2(-\omega) = ih(\omega) \frac{a_\omega^\dagger}{2}. \quad (24)$$

We now consider the system operators,  $A_k$ , and the eigen-spectrum of  $\tilde{H}_A$  being discrete with eigenvectors,  $|\psi_\epsilon\rangle$ , having

eigenvalues,  $\epsilon$ , we define an operator  $A_k(\omega)$ , given by

$$A_k(\omega) = \sum_{\epsilon' - \epsilon = \omega} |\psi_\epsilon\rangle \langle \psi_\epsilon | A_k | \psi_{\epsilon'}\rangle \langle \psi_{\epsilon'} |, \quad (25)$$

where  $k = 1$  or  $2$ . The eigenvalues and eigenstates of the transmon Hamiltonian,  $\tilde{H}_A$ , are respectively given by

$$\begin{aligned} \epsilon_n &= \tilde{\omega}_0 n - \tilde{\omega}_1 n^2, \\ |\psi_\epsilon\rangle &= \frac{b^{\dagger n}}{\sqrt{n!}} |\psi_0\rangle, \end{aligned} \quad (26)$$

where  $n$  denotes the  $n^{\text{th}}$  level of the transmon. So using equations (25) and (26), for  $n = n' + 1$ , using the commutation relation of the annihilation and creation operators, we obtain

$$A_1(\omega_{n'}) = \sqrt{n'+1} |\psi_{\epsilon_{n'+1}}\rangle \langle \psi_{\epsilon_{n'}} | = T_{\uparrow n'}. \quad (27)$$

where the dimensionless quantity,  $\omega_{n'} = \epsilon_{n'} - \epsilon_{n'+1} = -\omega_0 + 2\omega_1 n' + \omega_1$ . Whereas for  $n + 1 = n'$ , similarly we arrive at the expression

$$A_1(\omega_n) = \sqrt{n+1} |\psi_{\epsilon_n}\rangle \langle \psi_{\epsilon_{n+1}} | = T_{\downarrow n} \quad (28)$$

where the dimensionless quantity,  $\omega_n = \epsilon_{n+1} - \epsilon_n = \tilde{\omega}_0 - 2\omega_1 n - \tilde{\omega}_1$ . Therefore the energy differences associated with the allowed transitions,  $n \rightarrow n+1$  and  $n+1 \rightarrow n$  are  $\omega_n = -\tilde{\omega}_0 + 2\omega_1 n + \tilde{\omega}_1 = \omega_{\uparrow n} = -\omega_{\downarrow n}$  and  $\omega_n = \tilde{\omega}_0 - 2\omega_1 n - \tilde{\omega}_1 = \omega_{\downarrow n}$  respectively. Similarly, the operators corresponding to  $A_2$ , which are associated with the transitions  $n \rightarrow n+1$  and  $n+1 \rightarrow n$  are given by

$$\begin{aligned} A_2(\omega_{\uparrow n}) &= -i\sqrt{n+1} |\psi_{\epsilon_n}\rangle \langle \psi_{\epsilon_{n+1}} | = T_{\downarrow n} \text{ and} \\ A_2(\omega_{\downarrow n}) &= i\sqrt{n+1} |\psi_{\epsilon_{n+1}}\rangle \langle \psi_{\epsilon_n} | = T_{\uparrow n} \end{aligned} \quad (29)$$

respectively.

Now, to complete the description of the evolution of the charger and the battery, we seek the decay rates of the GKSL master equation (9). Following the exposition in [39], we see that the decay rates for each transition corresponding to the energy difference  $\omega_n$  are given by,

$$\gamma_{ij}(\omega_n) = 2\pi \text{Tr}[B_i(\omega_n) B_j \rho_B], \quad \forall i, j, \quad (30)$$

where  $\rho_B$  is the density matrix of the bath, which is considered to be a thermal state comprising of infinite number of harmonic oscillators.

Substituting the bath operators from the interaction term,  $\tilde{H}_{EA}$ , the decay rate for  $i, j = 1$  is given by

$$\begin{aligned} \gamma_{11}(\omega_n) &= 2\pi \text{Tr}[B_1(\omega_n) B_1 \rho_B] \\ &= 2\pi \int_0^{\omega_{max}} \tilde{h}(\omega) \tilde{h}(\omega_n) \text{Tr} \left[ \frac{a_\omega (a_\omega + a_\omega^\dagger)}{4} \rho_B \right] d\omega, \end{aligned} \quad (31)$$

where  $\omega_{max}$  denotes the cutoff frequency of the bath. This cutoff frequency is set to be sufficiently high so that the memory time of the bath  $\sim \omega_{max}^{-1}$ , is negligibly small. Explicitly calculating (31), we obtain

$$\gamma_{11}(\omega_n) = \frac{\pi}{2} \tilde{h}^2(\omega_n) [\bar{n}(\omega_n) + 1], \quad (32)$$

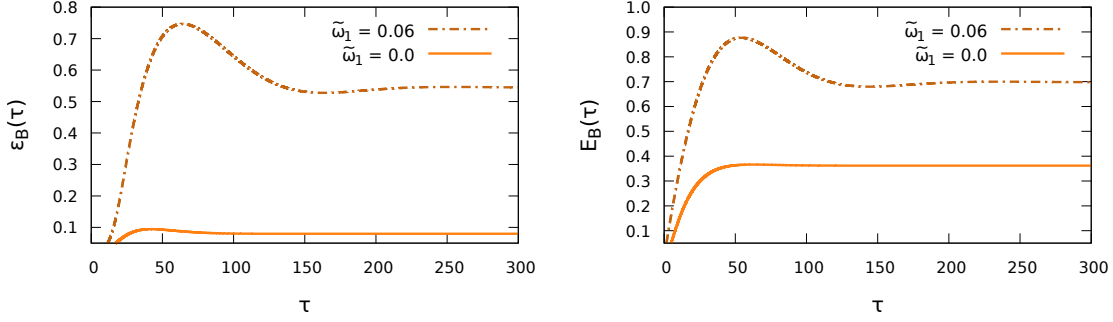


Figure 5. **Panel-(a):** Different curves correspond to the ergotropy versus interaction time for a fixed coherent drive  $F = 0.1$ . Dotted-dashed and solid curves respectively represent the energies of the anharmonic and harmonic oscillators, as a function of the interaction time. The parameters chosen are  $g = 0.1$ , the anharmonic oscillator frequencies as  $\tilde{\omega}_0 = 1.06$  and  $\tilde{\omega}_1 = 0.06$ . For the harmonic oscillator also,  $\tilde{\omega}_0 = 1.06$  is chosen. The quantities plotted along the horizontal axis is dimensionless, while ergotropy is in units of  $K$ . **Panel-(b):** Depiction of energy versus interaction time for the same set of values of the parameters. The quantities plotted along the horizontal axis is dimensionless, while energy is in units of  $K$ .

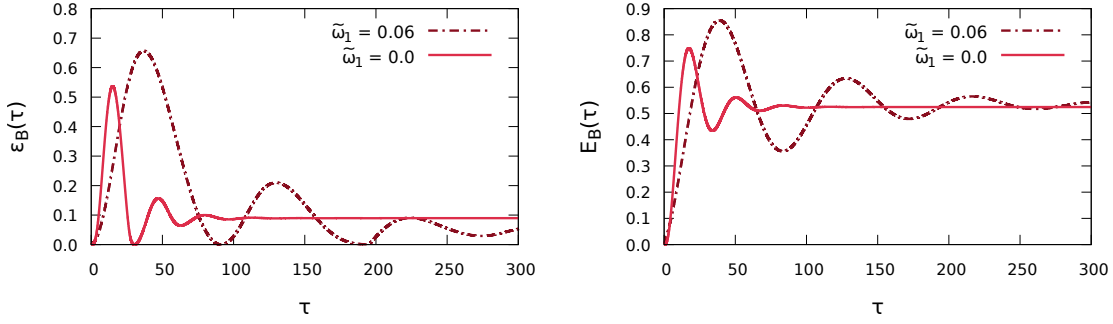


Figure 6. **Panel-(a):** Different curves correspond to the ergotropy versus interaction time for a fixed coherent drive  $F = 0.5$ . Dotted-dashed and solid curves respectively represent the energies of the anharmonic and harmonic oscillators, as a function of the interaction time. The parameters chosen are  $g = 0.1$ , the anharmonic oscillator frequencies as  $\tilde{\omega}_0 = 1.06$  and  $\tilde{\omega}_1 = 0.06$ . For the harmonic oscillator also,  $\tilde{\omega}_0 = 1.06$  is chosen. The quantities plotted along the horizontal axis is dimensionless, while ergotropy is in units of  $K$ . **Panel-(b):** Depiction of energy versus interaction time for the same set of values of the parameters. Quantities plotted along both axes are dimensionless. The quantities plotted along the horizontal axis is dimensionless, while energy is in units of  $K$ .

where  $J(\omega_n) = \tilde{h}^2(\omega_n)$ , is the spectral density of the bath at frequency  $\omega_n$ ,  $\bar{n}(\omega_n)$  is the mean number of bosons in the thermal state  $\rho_B$  of the bath with frequency  $\omega_n$ , which is given by  $\bar{n}(\omega_n) = [e^{\beta\omega_n/k_B} - 1]^{-1}$ , where  $\beta$  denotes the inverse temperature of the bath. Upon doing a similar calculation of the other elements of the decay rates, we obtain

$$\begin{aligned} \gamma(\omega_{\downarrow n}) &= \frac{\pi}{2} \tilde{h}^2(\omega_n) [\bar{n}(\omega_{\downarrow n}) + 1] \begin{pmatrix} 1 & -i \\ i & 1 \end{pmatrix} \text{ and,} \\ \gamma(-\omega_{\downarrow n}) &= \frac{\pi}{2} \tilde{h}^2(\omega_n) \bar{n}(\omega_{\downarrow n}) \begin{pmatrix} 1 & i \\ -i & 1 \end{pmatrix}. \end{aligned} \quad (33)$$

Now that we have everything we need for the master equation that describes the dynamics of the battery and charger, the GKSL master equation corresponding to Eq (7) for the battery

and charger is given by

$$\begin{aligned} \dot{\rho}_{AB}(t) &= -i[\sqrt{\tilde{\omega}}g(b\sigma^+ + b^\dagger\sigma^-) + \sqrt{\tilde{\omega}}F(b^\dagger + b), \tilde{\rho}_{AB}(t)] \\ &+ \sum_n \xi_n \left[ T_{\downarrow n} \tilde{\rho}_{AB}(t) T_{\uparrow n} - \frac{1}{2} \{T_{\downarrow n} T_{\uparrow n}, \tilde{\rho}_{AB}(t)\} \right] \\ &+ \sum_n \xi_n \left[ T_{\uparrow n} \tilde{\rho}_{AB}(t) T_{\downarrow n} - \frac{1}{2} \{T_{\uparrow n} T_{\downarrow n}, \tilde{\rho}_{AB}(t)\} \right], \end{aligned} \quad (34)$$

where  $\xi_n = 2\pi J(\omega_n) [\bar{n}(\omega_n) + 1]$ . For harmonic oscillator baths,  $\tilde{h}^2(\omega_n) = J(\omega_n)$ , where  $J(\omega_n)$  represents the spectral density function of the bath. The quantity  $J(\omega_n) = \tilde{\alpha} \omega_n \exp(-\omega_n/\omega_{max})$ . Here  $\alpha$  represents the dimensionless interaction strength between the anharmonic-oscillator and the bosonic bath. Here we have taken the interaction between the charger and battery to be linear. In contrast to the harmonic oscillator bath, in this scenario, we see that the annihilation and creation operators in the dissipative part of the GKSL master equation are replaced by  $n^{\text{th}}$  site transition op-



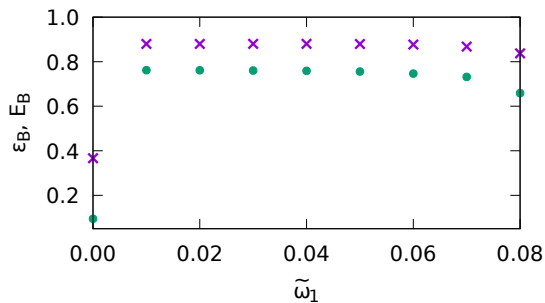


Figure 7. Demonstration of the maximum ergotropy and maximum energy obtainable as a function of the anharmonicity parameter,  $\tilde{\omega}_1$ . Teal circles denote the value of maximum energy,  $E_B(\tau)$  attained for different values of anharmonicity. The Purple crosses denote the same quantity, but for the case of the ergotropy  $\varepsilon_B(\tau)$ . Here we have obtained the results by setting  $g_1 = 0.1$ ,  $\gamma = 1.0$ ,  $F = 0.1$ , and we have set inverse temperature  $\beta = 1$ . The quantities plotted along the horizontal axis is dimensionless, while energy and ergotropy are in units of  $K$ .

erators, and we sum over all possible transitions of the anharmonic oscillator.

#### A. Does anharmonicity help in discharging?

Here we present the details of implementation of the dynamics of a two-level system as battery and an anharmonic charger, and we will study the resulting affect on maximum extractable energy from the battery using unitary operations. The dynamics of the anharmonic charger and the two-level battery (system  $B$ ) is governed by the master equation described in Eq. (34). We solve the master equation numerically using the Runge-Kutta method, to obtain  $\tilde{\rho}_{AB}$  as a function of interaction time, following which we discard the system  $A$ , and consider the system  $B$ .

In the case where there is no coherent driving, i.e.  $F = 0$ , our findings are in agreement with the expectation in that there is no ergotropy left on  $B$  while having a finite  $E_B(\tau)$ . Switching on the coherent drive  $F$  and increasing its value results in nonzero values of  $\varepsilon_B(\tau)$  that exhibit an oscillatory behavior that is a result of a competing effect between the dissipative and the coherent drive.

Fig. 5-(a) depicts the maximum extractable energy using unitary operations, i.e. the ergotropy, that is available from the quantum battery,  $B$ , as a function of the interaction time,  $\tau$ , if the charger is considered to be an anharmonic oscillator. We find that the amount of maximum extractable energy at all times is greater in the case where the charger is an anharmonic oscillator, than that of the harmonic oscillator case. Fig. 5-(a) is plotted for the values of the anharmonicity parameter,  $\tilde{\omega}_1 = 0.06$ , and the coherent driving strength,  $F = 0.1$ . This feature is also prevalent if we consider the energy of the battery,  $B$ , as a function of time. This implies that the amount of energy stored in the process of charging at any time of interaction, is higher in the case of anharmonic oscillator charger

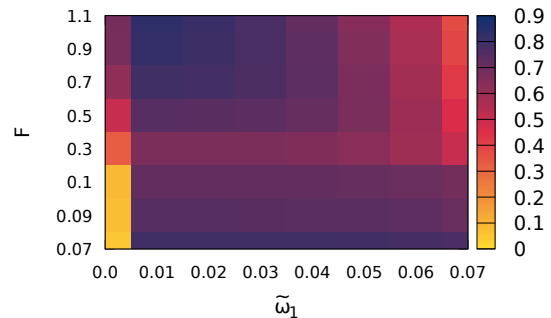


Figure 8. Depiction of the maximum ergotropy, where the maximization is performed over time, obtained for different values of the coherent drive intensity  $F$  along the vertical axis, and the anharmonic strength,  $\tilde{\omega}_1$ , along the horizontal axis. The quantities plotted along the horizontal and vertical axes are dimensionless, while ergotropy is in units of  $K$ .

than that for the harmonic oscillator case. Refer to Fig. 5-(b) for this. So using transmon as a charger is advantageous over using a simple harmonic oscillator in the process of charging or extracting maximal amount of energy from a quantum battery at all timescales, for a certain coherent drive.

For higher values of coherent drive strength, we find an advantage in the maximum ergotropy achieved over the interaction time, by using an anharmonic charger, over the harmonic one. However, the oscillatory behavior is increased for the anharmonic oscillator, and it takes a longer time to achieve a steady state. Refer to Fig. 6-(a). If we increase the value of the driving amplitude further, there is a drop in ergotropy value when compared to the harmonic oscillator case. We identify a range of values of the coherent drive strength for which there is an advantage in using an anharmonic charger instead of a harmonic one. Therefore, if there is a requirement of high values of ergotropy available at comparatively low timescales, then anharmonic chargers prove to be advantageous over harmonic ones. Qualitatively similar features are also present in the plot of energy extracted versus the interaction time. The maximum energy obtained over time is higher if we use an anharmonic charger, however it takes a longer time to achieve a steady state. Refer to Fig. 6-(b) for this.

We maximize the ergotropy and energy, separately over the timescale in which the system attains a steady state, and plot it with respect to the anharmonicity strength,  $\tilde{\omega}_1$ . We find that for certain values of coherent drive, there is a particular region of the anharmonicity strength where the maximum values of ergotropy and energy are higher if we use an anharmonic charger than that using a harmonic one. Refer to Fig. 7.

Intrigued by the complementarity that we obtained in the case of nonlinearity assisted charging, we try to find if any such feature also exists here. The heat map in Fig. 8 demonstrates the maximum ergotropy attained over time, for different values of the parameters,  $F$  and  $\tilde{\omega}_1$ . We find that, for a lower values of the coherent drive, the entire range of anharmonic strength,  $\tilde{\omega}_1$ , from 0.01 to 0.07, proves to be beneficial in the availability of maximal extractable energy. In

the case when the anharmonicity strength is 0, the maximum ergotropy is almost negligible for small values of coherent drive, and it increases slowly on increasing the driving strength. Moreover, at lower values of  $\tilde{\omega}_1 \sim 0.01$ , high values of the coherent drive  $\sim 1.0$  is required to attain the maximum ergotropy. Therefore we find that the anharmonicity in the charger is potentially useful in extracting energy maximally from a battery even for a small coherent drive.

## V. CONCLUSION

We have analyzed the effects of nonlinearities in the charger-battery system using an open-system approach. Specifically, we have studied two varieties of nonlinearities in the set-ups: non-linearly coupled charger and battery, and charger comprising an anharmonic oscillator which is linearly coupled to a two-level battery. In both the scenarios, the battery is not in direct contact of the environment and only the charger interacts with the environment and is acted on by a coherent drive. Before the external drive and the interaction with the environment is switched on, we began with the ground states of both the charger and battery.

In the case of nonlinearity in the coupling between charger and battery, we found that there is an enhancement in the steady-state ergotropy over the linear case. We also found in-

stances where the ergotropy in the transient state is zero in the linear case, but is positive for all non-zero values of the non-linear interaction strength. Further, we found that the times of attainment of maximum and steady-state ergotropies, where the maximization is over time, get reduced if we use non-linear interaction between charger and battery. We also found a complementarity between strengths of the nonlinear interaction and the coherent drive for obtaining the same steady-state ergotropy values.

We obtained the exact form of the master equation of the charger-battery system, when the charger is an anharmonic oscillator, and is connected to a bosonic Markovian environment. Considering the charger to be an anharmonic oscillator, for example a transmon, we found that there is a significant advantage in the maximum ergotropy over the linear setup, though the maximum is attained at a slightly later time for the anharmonic case. We also identified instances where the anharmonicity-assisted charging proves to be beneficial over the harmonic case, over all timescales. We separately maximized the ergotropy and energy, over the timescale in which the system attains a steady state, and found that for certain values of the coherent drive, there is a specific region of the anharmonicity strength where the maximum values of ergotropy and energy are higher in the case of an anharmonic charger than when using a harmonic one. Moreover, we observed a specific region of the parameter space of anharmonicity strength and coherent drive where the ergotropy values are maximum.

- 
- [1] J. Bardeen and W. H. Brattain, "Physical principles involved in transistor action," *Phys. Rev.* **75**, 1208–1225 (1949).
  - [2] G. L. Pearson and W. H. Brattain, "History of semiconductor research," *Proceedings of the IRE* **43**, 1794–1806 (1955).
  - [3] J. L. Bromberg, "The Birth of the Laser," *Physics Today* **41**, 26–33 (1988).
  - [4] J. Preskill, "Quantum Computing in the NISQ era and beyond," *Quantum* **2**, 79 (2018).
  - [5] N. Gisin and R. Thew, "Quantum communication," *Nature photonics* **1**, 165–171 (2007).
  - [6] R. Blatt and C. F. Roos, "Quantum simulations with trapped ions," *Nature Physics* **8**, 277–284 (2012).
  - [7] R. Alicki, "The quantum open system as a model of the heat engine," *Journal of Physics A: Mathematical and General* **12**, L103 (1979).
  - [8] S. Deffner and S. Campbell, "Quantum thermodynamics," Morgan & Claypool Publishers **10**, 2053–2571 (2019).
  - [9] J. Millen and A. Xuereb, "Perspective on quantum thermodynamics," *New J. Phys.* **18**, 011002 (2016).
  - [10] H. E. D. Scovil and E. O. Schulz-DuBois, "Three-level masers as heat engines," *Phys. Rev. Lett.* **2**, 262–263 (1959).
  - [11] R. Kosloff, "A quantum mechanical open system as a model of a heat engine," *The Journal of chemical physics* **80**, 1625–1631 (1984).
  - [12] D. Saha, A. Bhattacharyya, K. Sen, and U. Sen, "Harnessing energy extracted from heat engines to charge quantum batteries," (2023), [arXiv:2309.15634](https://arxiv.org/abs/2309.15634).
  - [13] R. Kosloff and A. Levy, "Quantum heat engines and refrigerators: Continuous devices," *Annual review of physical chemistry* **65**, 365–393 (2014).
  - [14] F. Clivaz, R. Silva, G. Haack, J. B. Brask, N. Brunner, and M. Huber, "Unifying paradigms of quantum refrigeration: A universal and attainable bound on cooling," *Phys. Rev. Lett.* **123**, 170605 (2019).
  - [15] M. T. Mitchison, "Quantum thermal absorption machines: Refrigerators, engines and clocks," *Contemporary Physics* **60**, 164–187 (2019).
  - [16] F. Campaioli, F. A. Pollock, F. C. Binder, L. Céleri, J. Goold, S. Vinjanampathy, and K. Modi, "Enhancing the charging power of quantum batteries," *Phys. Rev. Lett.* **118**, 150601 (2017).
  - [17] D. Ferraro, M. Campisi, G. M. Andolina, V. Pellegrini, and M. Polini, "High-power collective charging of a solid-state quantum battery," *Phys. Rev. Lett.* **120**, 117702 (2018).
  - [18] G. M. Andolina, D. Farina, A. Mari, V. Pellegrini, V. Giovannetti, and M. Polini, "Charger-mediated energy transfer in exactly solvable models for quantum batteries," *Phys. Rev. B* **98**, 205423 (2018).
  - [19] A. E. Allahverdyan, R. Balian, and T. M. Nieuwenhuizen, "Maximal work extraction from finite quantum systems," *Europhysics Letters* **67**, 565 (2004).
  - [20] M. Perarnau-Llobet, K. V. Hovhannissyan, M. Huber, P. Skrzypczyk, N. Brunner, and A. Acín, "Extractable work from correlations," *Phys. Rev. X* **5**, 041011 (2015).
  - [21] F. C. Binder, S. Vinjanampathy, K. Modi, and J. Goold, "Quantacell: powerful charging of quantum batteries," *New Journal of Physics* **17**, 075015 (2015).
  - [22] K. V. Hovhannissyan, M. Perarnau-Llobet, M. Huber, and A. Acín, "Entanglement generation is not necessary for optimal work extraction," *Phys. Rev. Lett.* **111**, 240401 (2013).

- [23] K. V. Hovhannisyanyan, M. Perarnau-Llobet, M. Huber, and A. Acín, “Entanglement generation is not necessary for optimal work extraction,” *Phys. Rev. Lett.* **111**, 240401 (2013).
- [24] T. P. Le, J. Levinsen, K. Modi, M. M. Parish, and F. A. Pollock, “Spin-chain model of a many-body quantum battery,” *Phys. Rev. A* **97**, 022106 (2018).
- [25] G. M. Andolina, M. Keck, A. Mari, M. Campisi, V. Giovannetti, and M. Polini, “Extractable work, the role of correlations, and asymptotic freedom in quantum batteries,” *Phys. Rev. Lett.* **122**, 047702 (2019).
- [26] A. Bhattacharyya, K. Sen, and U. Sen, “Noncompletely positive quantum maps enable efficient local energy extraction in batteries,” *Phys. Rev. Lett.* **132**, 240401 (2024).
- [27] R. Alicki and M. Fannes, “Entanglement boost for extractable work from ensembles of quantum batteries,” *Phys. Rev. E* **87**, 042123 (2013).
- [28] A. Crescente, M. Carrega, M. Sasseti, and D. Ferraro, “Charging and energy fluctuations of a driven quantum battery,” *New Journal of Physics* **22**, 063057 (2020).
- [29] A. C. Santos, A. Saguia, and M. S. Sarandy, “Stable and charge-switchable quantum batteries,” *Phys. Rev. E* **101**, 062114 (2020).
- [30] M. Carrega, A. Crescente, D. Ferraro, and M. Sasseti, “Dissipative dynamics of an open quantum battery,” *New Journal of Physics* **22**, 083085 (2020).
- [31] A. C. Santos, “Quantum advantage of two-level batteries in the self-discharging process,” *Phys. Rev. E* **103**, 042118 (2021).
- [32] V. Shaghghi, V. Singh, G. Benenti, and D. Rosa, “Micro-masers as quantum batteries,” *Quantum Science and Technology* **7**, 04LT01 (2022).
- [33] J. Gyhm, D. Šafránek, and D. Rosa, “Quantum charging advantage cannot be extensive without global operations,” *Phys. Rev. Lett.* **128**, 140501 (2022).
- [34] P. Chaki, A. Bhattacharyya, K. Sen, and U. Sen, “Auxiliary-assisted stochastic energy extraction from quantum batteries,” (2023), [arXiv:2307.16856](https://arxiv.org/abs/2307.16856).
- [35] P. Chaki, A. Bhattacharyya, K. Sen, and U. Sen, “Positive and non-positive measurements in energy extraction from quantum batteries,” (2024), [arXiv:2404.18745](https://arxiv.org/abs/2404.18745).
- [36] Donato Farina, Gian Marcello Andolina, Andrea Mari, Marco Polini, and Vittorio Giovannetti, “Charger-mediated energy transfer for quantum batteries: An open-system approach,” *Phys. Rev. B* **99**, 035421 (2019).
- [37] C. A. Downing and M. S. Ukhtary, “A quantum battery with quadratic driving,” *Communications Physics* **6**, 322 (2023).
- [38] H. P. Breuer and F. Petruccione, *The theory of open quantum systems* (Oxford University Press, Great Clarendon Street, 2002).
- [39] A. Rivas and S. F. Huelga, “Open quantum systems. an introduction,” <https://arxiv.org/abs/1104.5242>, [arXiv:1104.5242](https://arxiv.org/abs/1104.5242).
- [40] J. M. Martinis, S. Nam, J. Aumentado, and C. Urbina, “Rabi oscillations in a large josephson-junction qubit,” *Phys. Rev. Lett.* **89**, 117901 (2002).
- [41] John M. Martinis, K. B. Cooper, R. McDermott, Matthias Steffen, Markus Ansmann, K. D. Osborn, K. Cicak, Seongshik Oh, D. P. Pappas, R. W. Simmonds, and Clare C. Yu, “Decoherence in josephson qubits from dielectric loss,” *Phys. Rev. Lett.* **95**, 210503 (2005).
- [42] G. Wendin, “Quantum information processing with superconducting circuits: a review,” *Reports on Progress in Physics* **80**, 106001 (2017).
- [43] D. Farina, G. M. Andolina, A. Mari, M. Polini, and V. Giovannetti, “Charger-mediated energy transfer for quantum batteries: An open-system approach,” *Phys. Rev. B* **99**, 035421 (2019).
- [44] S. Felicetti, D. Z. Rossatto, E. Rico, E. Solano, and P. Forn-Diaz, “Two-photon quantum rabi model with superconducting circuits,” *Physical Review A* **97**, 013851 (2018).
- [45] S. Felicetti, J. S. Padernales, I. L. Egusquiza, G. Romero, L. Lamata, D. Braak, and E. Solano, “Spectral collapse via two-phonon interactions in trapped ions,” *Physical Review A* **92**, 033817 (2015).
- [46] A. Delmonte, A. Crescente, M. Carrega, D. Ferraro, and M. Sasseti, “Characterization of a two-photon quantum battery: Initial conditions, stability and work extraction,” *Entropy* (2021), 10.3390/e23050612, [arXiv:2105.08337v1](https://arxiv.org/abs/2105.08337v1).
- [47] A. Crescente, M. Carrega, M. Sasseti, and D. Ferraro, “Ultrafast charging in a two-photon dicke quantum battery,” *Phys. Rev. B* **102**, 245407 (2020).
- [48] R. Alicki and K. Lendi, *Quantum Dynamical Semigroups and Applications* (Springer, Berlin Heidelberg, 2007).
- [49] D. A. Lidar, “Lecture notes on the theory of open quantum systems,” (2020), [arXiv:1902.00967](https://arxiv.org/abs/1902.00967).
- [50] A. Kossakowski, “On quantum statistical mechanics of non-hamiltonian systems,” *Reports on Mathematical Physics* **3**, 247–274 (1972).
- [51] V. Gorini, A. Kossakowski, and E. C. G. Sudarshan, “Completely positive dynamical semigroups of n-level systems,” *Journal of Mathematical Physics* **17**, 821–825 (1976).
- [52] G. Lindblad, “On the generators of quantum dynamical semigroups,” *Communications in Mathematical Physics* **48**, 119–130 (1976).
- [53] D. Manzano, “A short introduction to the lindblad master equation,” *AIP Advances* **10** (2020), 10.1063/1.5115323.
- [54] P. Skrzypczyk, R. Silva, and N. Brunner, “Passivity, complete passivity, and virtual temperatures,” *Phys. Rev. E* **91**, 052133 (2015).
- [55] M. Perarnau-Llobet, K. V. Hovhannisyanyan, M. Huber, P. Skrzypczyk, J. Tura, and A. Acín, “Most energetic passive states,” *Phys. Rev. E* **92**, 042147 (2015).
- [56] E. G. Brown, N. Friis, and M. Huber, “Passivity and practical work extraction using gaussian operations,” *New Journal of Physics* **18**, 113028 (2016).
- [57] C. Sparaciari, D. Jennings, and J. Oppenheim, “Energetic instability of passive states in thermodynamics,” *Nature Communications* **8** (2017).
- [58] M. Onuma-Kalu and R. B. Mann, “Work extraction using gaussian operations in noninteracting fermionic systems,” *Phys. Rev. E* **98**, 042121 (2018).
- [59] A. Lenard, “Thermodynamical proof of the Gibbs formula for elementary quantum systems,” *Journal of Statistical Physics* **19**, 575 (1978).
- [60] W. Pusz and S. L. Woronowicz, “Passive states and KMS states for general quantum systems,” *Communications in Mathematical Physics* **58**, 273 (1978).
- [61] Y. Nakamura, Y. Pashkin, and J. Tsai, “Coherent control of macroscopic quantum states in a single-cooper-pair box,” *Nature* **398**, 786–788 (1999).
- [62] J. Koch, T. M. Yu, J. Gambetta, A. A. Houck, D. I. Schuster, J. Majer, A. Blais, M. H. Devoret, S. M. Girvin, and R. J. Schoelkopf, “Charge-insensitive qubit design derived from the cooper pair box,” *Phys. Rev. A* **76**, 042319 (2007).
- [63] M. H. Devoret, “Quantum fluctuations,” in *Les Houches Session LXIII*, edited by S. Reynaud, E. Giacobino, and J. Zinn-Justin (Elsevier, New York, 1997) pp. 351–386.
- [64] U. Vool and M. Devoret, “Introduction to quantum electromagnetic circuits,” [10.1002/cta.2359](https://arxiv.org/abs/10.1002/cta.2359).